Modelling the Distribution of Lasers in Biological Tissues

Teodora Petrova*, Zhivo Petrov

Faculty of Aviation, Vasil Levski National Military University
Town of Dolna Mitropoliya, District Pleven, Bulgaria
E-mails: teodorapetrova33@abv.bg, zhbpetrov@nvu.bg

**Corresponding author*

Received: May 30, 2017 **Accepted: August 30, 2018**

Published: September 30, 2018

Abstract: *For the time being there is no accurate theory about the spread of light in a structurally non-homogeneous medium whereas the experimental research is additionally hindered because of the necessity to maintain constant structural-dynamic parameters. In this respect numerical modelling of the processes of spreading of laser radiation plays increasingly important role.*

Keywords: *Biomedical technologies, Lasers, Mathematical model.*

Introduction

For the time being there is no accurate theory about the spread of light in a structurally non-homogeneous medium whereas the experimental research is additionally hindered because of the necessity to maintain constant structural-dynamic parameters. The question of the interaction of laser radiation with multilayer biological materials is of particular interest. In this respect computer modelling of the processes of distribution of laser radiation plays increasingly important role. It allows more detailed exploration of the specific aspects of the process of distribution of a laser beam in a modelled medium and to study the relation between the achieved results from different parameters of a measurement system and the scrutinized item, which always encumbers the experiment additionally. With the new areas of laser radiation application for the treatment of bio-tissues constantly emerging, the necessity to develop a methodology and criteria for the optimization of the parameters of laser emitters arises [3, 7, 13].

Optimisation of the laser radiation parameters

Bio-tissues are a multi-component material, which contains mainly protein (collagen), fats, minerals and water. Each of these constituents has a different coefficient of absorption, thermal conductivity and temperature conductivity [1, 8]. Different mathematical models have been developed for these purposes; those models are usually designed to solve a particular problem. In most of the cases the problem is the choice of a laser and its properties; the solution is based on the spectral absorption and time for recovery of the scrutinized item (medium). The modelling should solve the problem for optimization of the parameters of a laser emitter and assessment of the achieved results from the laser impacts of the laser already selected on the biological medium [16].

Through the model defining a specific process and basing on the results from the impact under certain parameters, the input parameters can be gradually changed by having optimized the energy parameters of the laser emitter so that needed effect in each specific case could be achieved.

Interesting results were obtained by stochastic modelling through the Monte-Carlo method of processes of repeated scattering of laser beams in a multi-layer medium [4, 11, 12]. The Monte-Carlo method is a digital method for solving mathematical problems (systems of algebraic, differential, integral equations) and direct statistical modelling (physical, chemical, biological, economic and social processes) with the help of obtaining and modifying random digits.

The main idea of the method is to consider the effect of absorption and scattering of the optical path of each photon through non-transparent medium. For the absorption to be taken into account, each photon needs to acquire weight and when the photon goes through the medium that weight stays constant and does not change. If there is scattering, then a new direction of propagation is chosen in accordance with the phase function and other random digits. The procedure continues until the photon gets out of the scrutinized volume or its weight assumes a certain measure. The Monte-Carlo method has five major stages, namely:

1. Photon source generation – a photon is generated on the surface of the studied medium. Its spatial and angular distribution corresponds to the distribution of the incident radiation.
2. Generation of trajectory – having generated the photon, the distance to the first collision is determined by assuming that the particles that are absorbed are randomly distributed in a non-transparent medium.
3. Absorption – to be able to assess the absorption, each photon is given weight and when the photon enters into the non-transparent medium its weight is equal to 1.
4. Destruction – this step is used only in case when assigning the weight to each photon at stage 3. When the weight acquires certain border value, the photon is eliminated. Then the programme goes on from stage 1.
5. Registration – after the repetition of stages 1-4 for sufficient quantity of photons, the trajectory map is calculated and kept in the computer. In this way, statistically we can consider parts of random photons absorbed by the medium and the spatial and angular distribution of the photons emerging out of it [2, 5].

One of the options to implement the algorithm under the Monte-Carlo method is by simulating a medium of the following parameters: thickness L_{cp}, scattering coefficient μ_c, and absorption coefficient μ_a, average cosine of the angle of scattering g, relative refractive index n. The medium is shown as a sum of centres that scatter and absorb photons [9, 10, 17].

The algorithm of the implementation of the Monte-Carlo method is given in Fig. 1.

We can track an iteration of an algorithm under the Monte-Carlo method in details (Fig. 1). The incident impulse that consists of one million photons getting into the investigated medium along the z axis perpendicular to the surface (x, y) as they intersect it at point with coordinates (0, 0, 0). All calculations are carried out for a three-dimensional Cartesian coordinate system. After the photon enters the medium, the mean free path of the photon in the medium and the scattering angles θ and φ are determined. The scattering angle θ is defined by the phase function of scattering

$$p(s,s') = p(\theta)\,p(\varphi), \tag{1}$$

where s is the incident direction and s' – the direction of photon scattering.

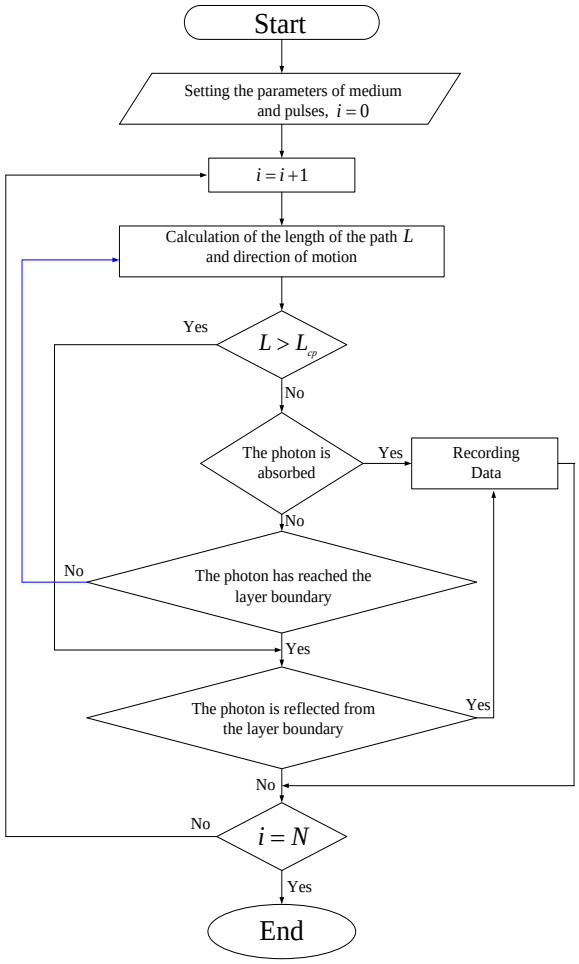

Fig. 1 Algorithm of the implementation of the Monte-Carlo method

The particles of the surrounding medium due to which scattering and absorption take place are assumed to be spherically symmetrical. This approximation is often used in similar cases and is based on the fact that during the process of passage through the medium with strong scattering of photons interacts with the particles under different angles. Therefore, we can apply averaging of the scattering indicatrix. The application of that model shows that this approximation manifests the properties of most of the bio-tissues quite well [9, 10, 17].

From this assumption, we can write the following correlation

$$p(\varphi) = \frac{1}{2\pi}. \tag{2}$$

When the tissues have strong scattering, for the scattering phase function $p(\theta)$ can be applied the Henie-Greenstein's phase function from which for the θ angle we obtain:

$$\theta = \cos^{-1}\left[\frac{1+g^2-\left(\frac{1-g^2}{1+g^2-2gRND}\right)}{2g}\right], \tag{3}$$

where RND is a random uniformly distributed number in the range (0, 1).

At each stage the angle θ is determined in relation to the "old" direction of propagation while the angle φ is in a medium that is perpendicular to the "new" direction of movement. The length of the free path of the photon is assessed from the probability density function:

$$p(L)=\left(\frac{1}{l_{ph}}\right)e^{-\frac{L}{l_{ph}}}, \tag{4}$$

where l_{ph} is the average length of free path of the photon and is determined by the expression

$$l_{ph}=\frac{1}{\mu_a+\mu_s}. \tag{5}$$

Having applied the property of the probability density function

$$\int_0^{\infty} p(L)dL=1 \tag{6}$$

to calculate the length of the free path, a random number $\xi \in (0, 1)$ is chosen, which can be linked to the probability density of the length of free path in the following manner:

$$\xi=\int_0^{L} p(l)dl. \tag{7}$$

The number ξ is uniformly distributed in the interval (0, 1) and is generated with the help of a random numbers generator. Then the length of free path of the photon is acquired through:

$$L=-l_{ph}\ln(1-\xi). \tag{8}$$

Using the generated digit ξ the interaction of the photon with the particles of the medium is modelled; the particles can be either absorbing or of scattering centres. The probability of a photon to be scattered by the particles is assessed through the expression:

$$p_s=\frac{\mu_s}{\mu_s+\mu_a} \tag{9}$$

and the probability of absorption is:

$$p_a=1-p_s=\frac{\mu_a}{\mu_s+\mu_a}. \tag{10}$$

When the generated random number ξ is in the range (0, p_s) we assume that the photon is scattered; otherwise we assume that it is absorbed. The total medium along the *z*-axis is virtually divided into a number of layers of equal thickness and they correspond to data arrays. The numbers of the absorbed or scattered photons are recorded in each array. If the photon is scattered, its new direction of movement and its coordinates are calculated under the following formulas:

$$x = x_0 + L\sin\theta\cos\varphi,$$
$$y = y_0 + L\sin\theta\sin\varphi, \quad (11)$$
$$z = z_0 + L\cos\theta,$$

where x_0, y_0, z_0 are the "old" coordinates of the photon.

If the photon is absorbed, the next photon is released at a point with coordinates (0, 0, 0). The process of modelling of the interaction of the photon with the particles of the medium continues until the photon is either absorbed or unless it goes out of the boundaries of the detectors ($z = 0$), or gets into it ($z = L_{cp}$). When the photon gets to the boundary of the medium-air, it is checked whether the condition of total internal reflection is fulfilled:

$$\theta \geq \theta_{kp} = \arcsin\left(\frac{1}{n}\right), \quad (12)$$

where n is the refractive index of medium.

Characteristics of the Monte-Carlo method:

- ✓ Convergence of the solution same as $1/N$.
- ✓ The dependence of the error on the number of iterations is also $\approx 1/\sqrt{N}$ and in order to reduce the error it is necessary to increase the number of iterations twice.
- ✓ The main method for reducing the errors remains the maximum variance reduction.
- ✓ The error does not affect the dimension of the problem.
- ✓ Simple structure of the computational algorithm, as the calculation of the realization of random variables is repeated N times.
- ✓ The construction of random variables can be based on the physical nature of the process and it is not necessarily required, as in the classical methods, to formulate the equation which is becoming increasingly topical for contemporary problems [6].

The main idea of the method is to trace the process of absorption and scattering throughout the entire optical path of a photon in an opaque environment. The distance between two collisions is selected from a logarithmic distribution, which uses random numbers generated by a computer. For an absorption to be taken into account, each photon is assigned a weight and by passing through the medium this weight permanently reduces. If there is scattering, then a new direction of propagation is chosen in accordance with the phase function and other random number. This procedure continues as long as the photon does not come out of the concerned area or its weight reaches a certain value [18].

Biological objects can be divided by their optical characteristics into highly scattering media that are optically opaque, such as skin, muscle, brain, blood, etc., and low scattering or transparent media such as the cornea and the lens of the eye. Laser therapy is associated with a nonspecific thermal impact on biological objects. The distribution of temperature determines the extent of impact on the tissue being treated and the level of thermal shock of the surrounding tissues, which must be reduced to minimum.

The study was carried out for the biological structures liver, blood and muscle tissue. The optical characteristics of human bio-tissues were measured *in vitro* and are shown in Table 1 [14, 15].

Table 1. Optical properties of bio-tissues

Bio-tissue	λ, nm	μ_a, cm^{-1}	μ_S, cm^{-1}	g
Liver	630	3.2	414	0.95
Blood	600	25	464	0.99
Muscle tissue	1064	2.0	215	0.96

The results from the modelling of the distribution of the density of the photons transmission in the liver are shown in Figs. from 2 to 6.

Fig. 2a shows the dependence of the density of the photons transmission, expressed in decibels, according to the penetration depth (on the *z* axis) and the radius of the distance from the *z* axis. The modelling was performed for a single beam entering into the tissue at a point with coordinates (0, 0, 0).

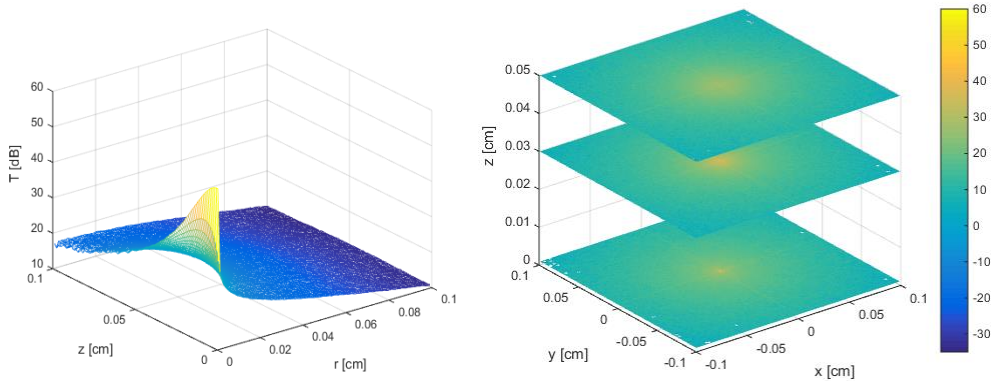

a) b)

Fig. 2 Single beam in liver

The results indicate that the density decreases with the increase of the penetration depth, while at the same time scattering of the beam is observed. Fig. 2b shows the density of transmission in three cross-sections of the tissue at depths of 0 cm, 0.03 cm and 0.05 cm. The expansion of the beam during the penetration into the tissue and the reducing of its intensity can be clearly seen. At a depth of 0.05 cm the beam is highly diffused and its intensity is significantly decreased, which determines that its efficiency will be low at greater depths.

Fig. 3 shows the results of the modelling for a uniform beam with a radius of 0.1 cm, with coordinates of its center during penetration into the tissue (0, 0, 0).

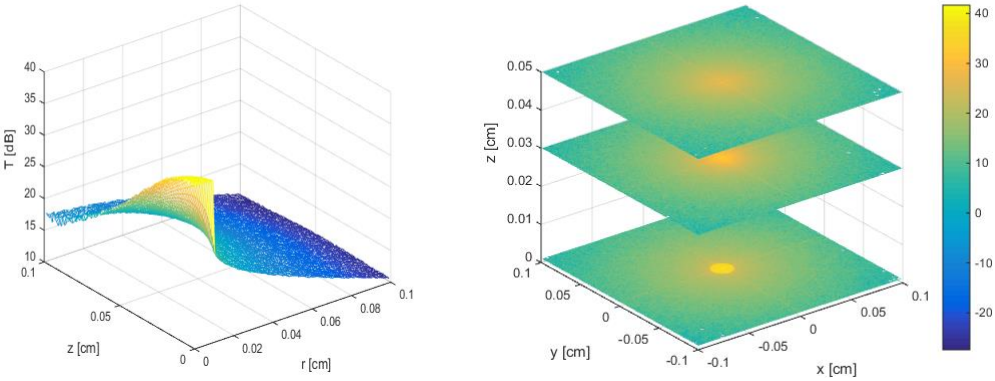

a) b)

Fig. 3 Uniform beam with a radius of 0.1 cm in liver

Fig. 3a shows the results for the density of the transmission of photons, expressed in decibels, depending on the penetration depth (on the *z* axis) and the radius of the distance from the *z* axis. The larger radius of the beam during the distribution in the tissue compared to the single beam can also be clearly observed. The speed with which the density of the transmission of photons in depth decreases is lower than in the single beam. Fig. 3b shows the density of the transmission in three sections. On the entry surface of the tissue the spot of the beam can be clearly distinguished. A visible expansion of the beam in the next two sections is observed.

Fig. 4 shows the results of the modelling for a Gaussian beam with a radius of 0.1 cm, with coordinates of its center during penetration into the tissue (0, 0, 0).

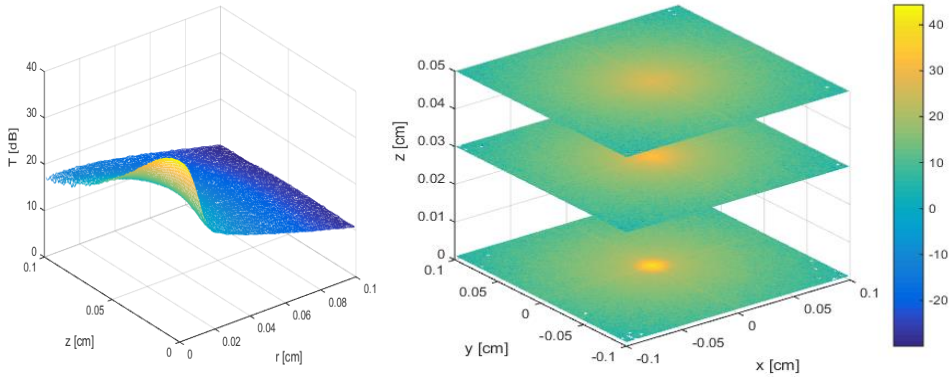

a) b)

Fig. 4 Beam with a Gaussian distribution and a radius of 0.1 cm in liver

From the results for the density of the transmission of photons, depending on the penetration depth (on the *z* axis) and the radius of the distance from the *z* axis (Fig. 4a) can be seen that the density level along the width of the tissue is higher compared to the cases considered above. The alteration in the density from the penetration depth does not differ substantially from the case of the uniform beam. Fig. 4b shows the transmission density in the three cross-sections of the tissue. From the results, it can be concluded that the distribution of the photons is similar to the distribution during the use of a uniform beam. The main difference is in the greater width of the beam during its distribution in the tissue.

Fig. 5 shows the results of the modelling for focused Gaussian beam with a radius of 0.1 cm, depth of focus 0.03 cm and coordinates of its center during penetration into the tissue (0, 0, 0).

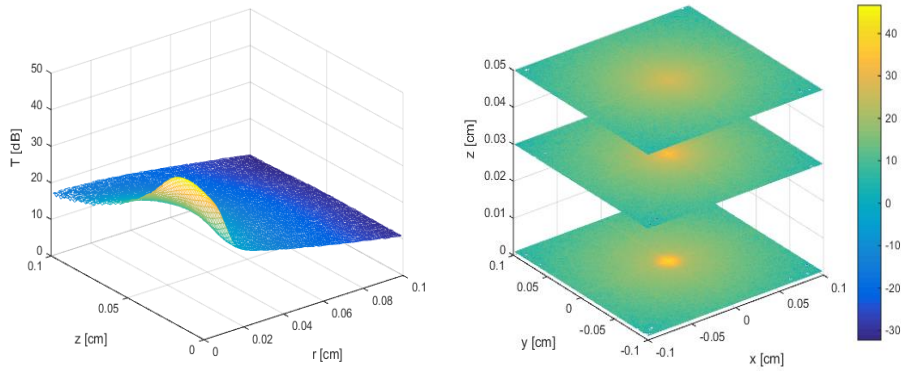

a) b)

Fig. 5 Focused Gaussian beam in liver

From the distribution of the density of photons transmission (Fig. 5a) depending on the depth of penetration (on the *z* axis) and the radius of the distance from the *z* axis, there are no differences with the case of the unfocused Gaussian beam. The analysis of the results from the penetration at different depths (Fig. 5b) indicates that the beam is focused at the depth of 0.03 cm (the width of the beam at this depth is less than at the entrance of the tissue). After this depth the beam quickly scatters and the distribution processes do not differ from those of the unfocused Gaussian beam. The possibility to achieve focusing of the beam inside the tissue allows reaching the greatest impact on a specific area of the tissue, which would increase the efficiency of the laser use.

Fig. 6 shows the contours with density levels of photons transmission in liver 37 dB, 30 dB, 27 dB, 23 dB and 13 dB for a single beam, a uniform beam with a radius of 0.1 cm, a beam with Gaussian distribution of 0.1 cm and a focused Gaussian beam depending on the penetration depth (on the *z* axis) and the radius of the distance from the *z* axis.

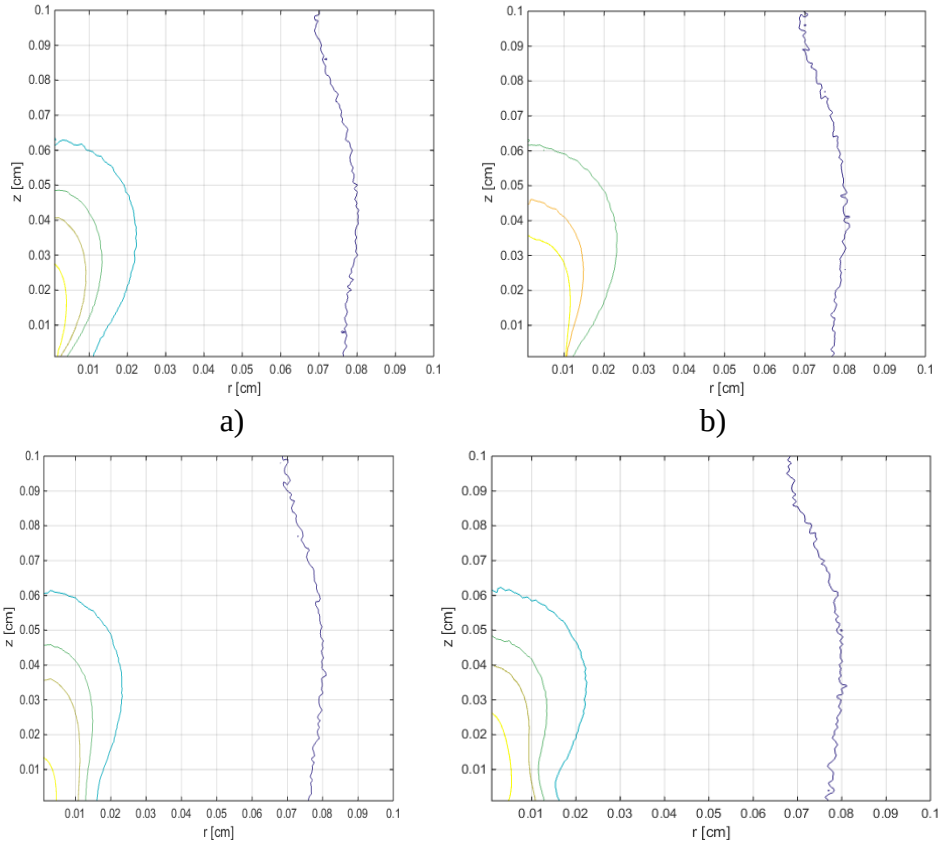

Fig. 6 Density distribution of the photons transmission in liver of:
a) a single beam; b) a uniform beam with a radius of 0.1 cm;
c) a beam with a Gaussian distribution and radius of 0.1 cm; d) a focused Gaussian beam.

From the analysis of the results it can be concluded that during the penetration into the tissue, the scattering when using a single beam is lowest. Such a beam is impossible to implement in practice but the results for it make it possible to determine which of the other types of beams has the closest type of distribution to it. From the results obtained it can be seen that the beam with a uniform distribution penetrates with the highest intensity, but at the same time it is also the widest. The unfocused Gaussian beam is with a smaller width but its intensity is smaller

than that of the uniform beam at greater depths. Closest to the manner of distribution of the single beam is the focused Gaussian beam.

A modelling of the distribution of the density of photons transmission in the considered types of beams in blood has been made and the results are shown in Figs. from 7 to 11. Fig. 7a shows the dependence of the density of the transmission of photons in blood, expressed in decibels, depending on the penetration depth (on the *z* axis) and the radius of the distance from the *z* axis for a single beam.

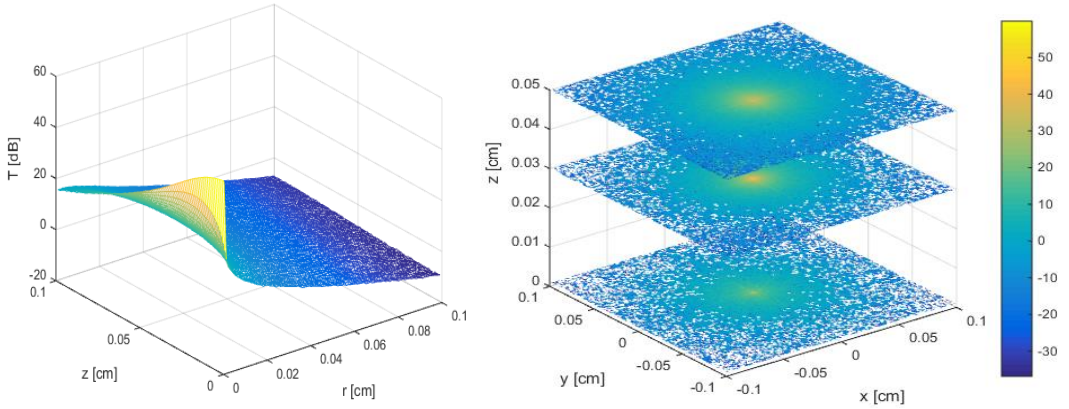

a) b)

Fig. 7 Single beam in blood

The results show that the decrease of the density of the transmission reduces considerably faster with the increasing of the radius r as compared to the penetration in the liver. Fig. 7b shows transmission density in the three cross-sections of the tissue. It can be seen that the beam is well defined even at a depth of 0.05 cm. The results obtained show that the density of the transmission is significantly lower on the side walls of the tissue than in penetration in the liver.

Fig. 8a shows the dependence of the density of the transmission of photons in the blood, expressed in decibels, according to the penetration depth (on the *z* axis) and the radius of the distance from the *z* axis for a uniform beam.

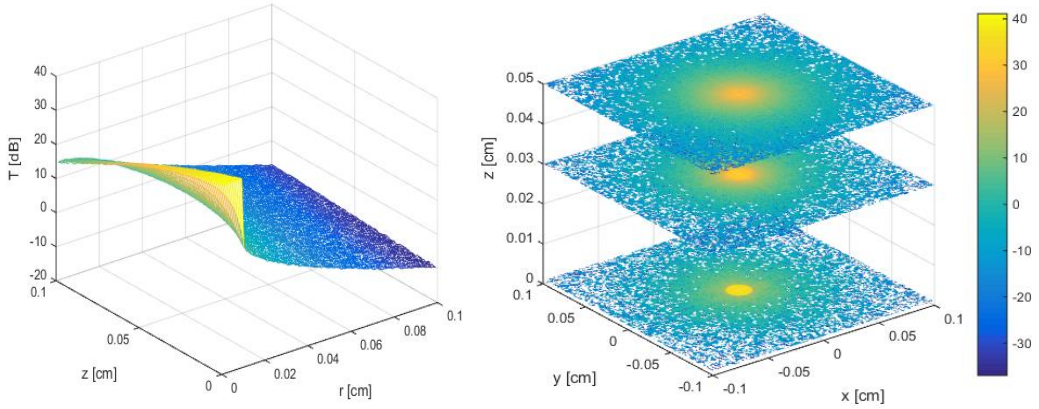

a) b)

Fig. 8 Uniform beam with a radius of 0.1 cm in blood

From the results obtained the same conclusions can be drawn as for the single beam. The results of the analysis for the three selected sections (Fig. 8b) indicate that in this beam

the observed scattering is also significantly less than in the liver. Despite the expansion, the shape of the beam is still well defined at different depths.

Fig. 9a shows the dependence of the density of the photons transmission in blood, expressed in decibels, according to the penetration depth (on the *z* axis) and the radius of the distance from the z axis for a Gaussian beam.

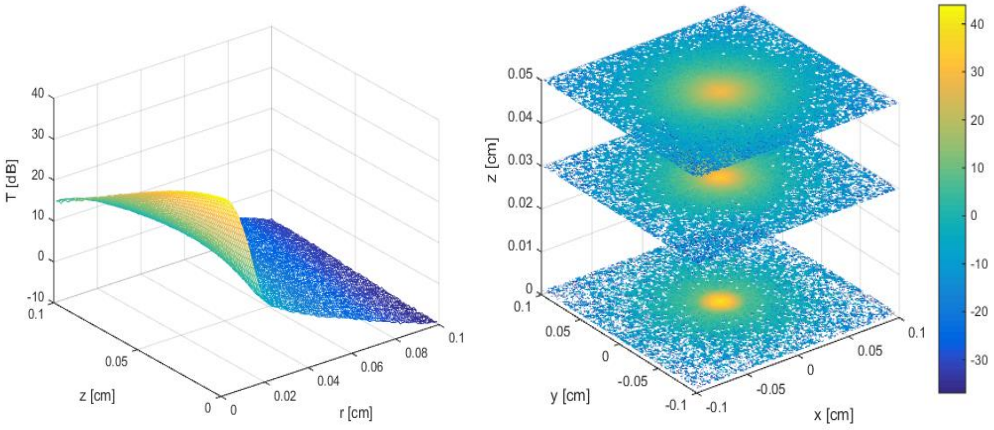

a) b)

Fig. 9 Beam with a Gaussian distribution of 0.1 cm in blood

The results show that the density of the transmission decreases more rapidly with depth than in the uniform beam. Fig. 9b shows transmission density in the three cross-sections of the tissue. There is an expansion of the beam during the penetration into the tissue but its intensity in the area around the axis is greater than during the penetration into the liver. On the figure, the well-shaped spot of the beam is clearly distinguished at all three depths.

Fig. 10a shows the dependence of the density of the transmission of photons in the blood, expressed in decibels, according to the penetration depth (on the *z* axis) and the radius of the distance from the *z* axis of a focused Gaussian beam.

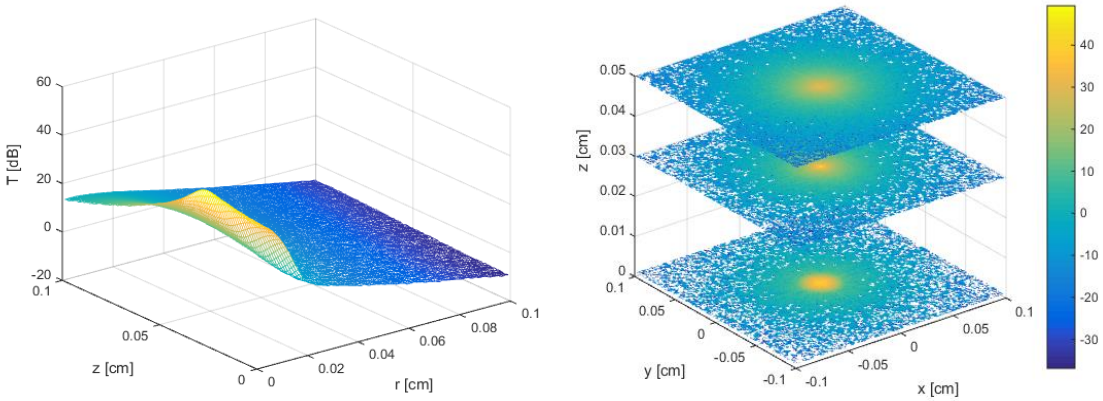

a) b)

Fig. 10 Focused Gaussian beam in blood

The results indicate a greater focus of the flow around the *z* axis. The analysis of the results for the three cross-sections of the tissue (Fig. 10b) shows the focusing of the beam in tissue penetration, the width of the beam spot at a depth of 0.03 cm being smaller, both, than the width at the penetration boundary of the beam and that at a depth of 0.05 cm.

Upon penetration of the focused Gaussian beam, significantly less scattering than in the penetration into the liver is observed.

Fig. 11 shows the density contours of the photons transmission in blood with levels 37 dB, 30 dB, 27 dB, 23 dB and 13 dB for a single beam, a uniform beam with a radius of 0.1 cm, a beam with Gaussian distribution of 0.1 cm and a focused Gaussian beam depending on the penetration depth (on the *z* axis) and the radius of the distance from the *z* axis.

The comparison of the results obtained with those in Fig. 6 confirms the conclusion drawn so far that the scattering of the beams in blood is significantly lower than that in liver.

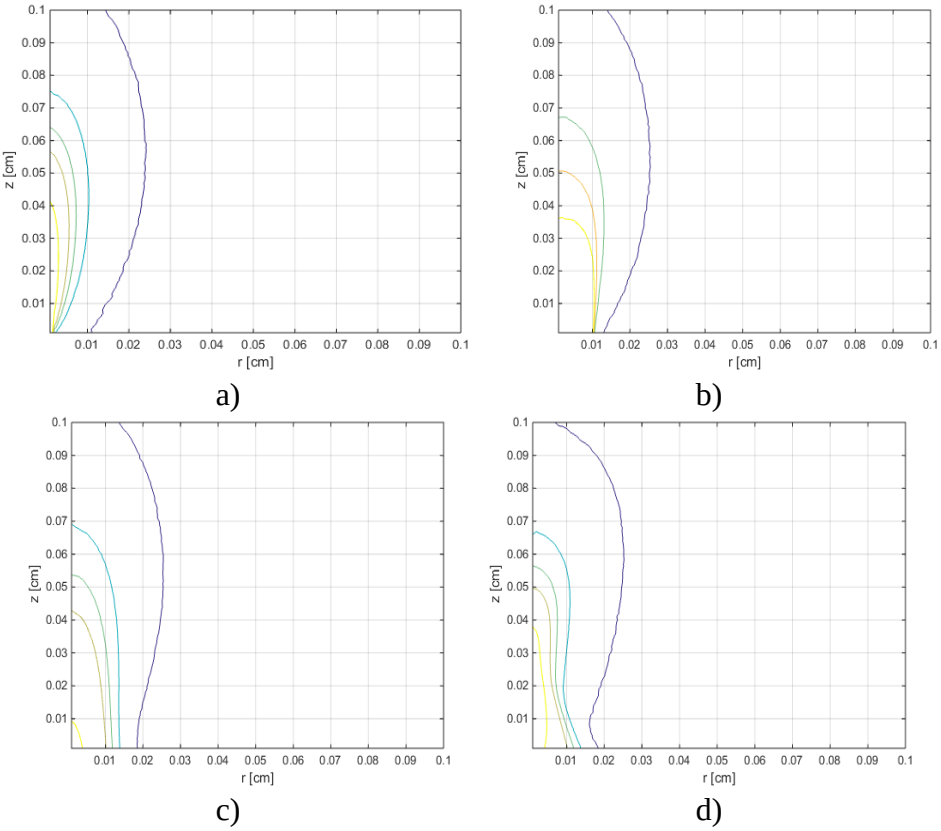

Fig. 11 Density distribution of photons transmission in blood of:
a) a single beam; b) a uniform beam with a radius of 0.1 cm;
c) a beam with a Gaussian distribution and a radius of 0.1 cm; d) a focused Gaussian beam.

Fig. 11d clearly shows how the beam initially narrows, and then there is an interval of depths at which it almost does not change its width and after a depth of 0.035 cm begins to expand. The results obtained indicate that upon penetration in the blood, the focused Gaussian beam is closest to the single beam.

The density distribution of the photons transmission in muscle tissue for the same types of beams is studied and the results are shown in Figures from 12 to 16. Fig. 12a shows the dependence of the density of the transmission of photons in muscle tissue, expressed in decibels, according to the penetration depth (on the *z* axis) and the radius of the distance from the *z* axis. The modelling was performed for a single beam entering into the tissue at a point with coordinates (0, 0, 0).

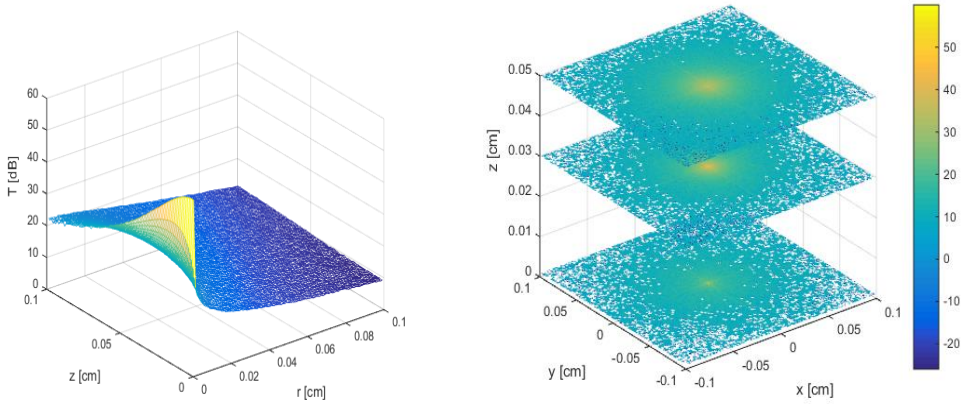

a) b)

Fig. 12 Single beam in muscle tissue

From the results it can be concluded that the decrease in density with the increase of penetration depth is greater in comparison with the penetration into the blood, but less than in the liver. The observed scattering of the beam is greater as compared to the penetration in the blood but less than in the liver. Fig. 12b shows the density of the transmission in the same three cross-sections of the tissue. The greater expansion of the beam upon penetration in the tissue compared with blood can be clearly seen. At a depth of 0.05 cm the beam is highly scattered and its intensity is significantly lowered which determines that its efficiency will be low at greater depths.

Fig. 13a shows the dependence of the density of the photons transmission in muscle tissue, expressed in decibels, according to the penetration depth (on the *z* axis) and the radius of the distance from the *z* axis. The modelling was performed for a uniform beam with a radius of 0.1 cm, entering into the tissue at a point with coordinates (0, 0, 0).

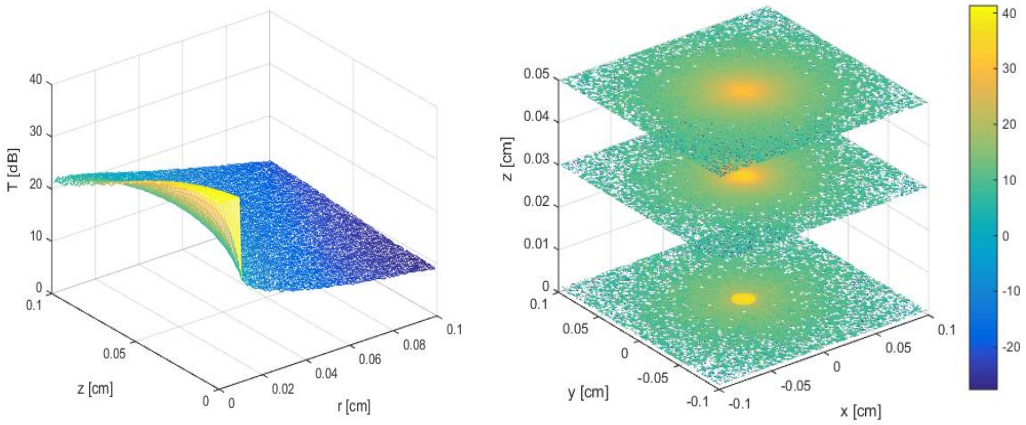

a) b)

Fig. 13 Uniform beam with a radius of 0.1 cm in muscle tissue

The results indicate that the density decreases with the penetration depth and at the same time scattering of the beam is observed. Fig. 13b shows the density of the transmission in the three cross-sections of the tissue. Despite the visible scattering, the form of the beam is clearly discernible in all three sections.

Fig. 14a shows the dependence of the density of the transmission of photons in the muscle tissue, expressed in decibels, according to the penetration depth (on the *z* axis) and the radius of the distance from the *z* axis. The modelling was performed for a beam with a Gaussian

distribution and a radius of 0.1 cm, entering into the tissue at a point with coordinates (0, 0, 0).

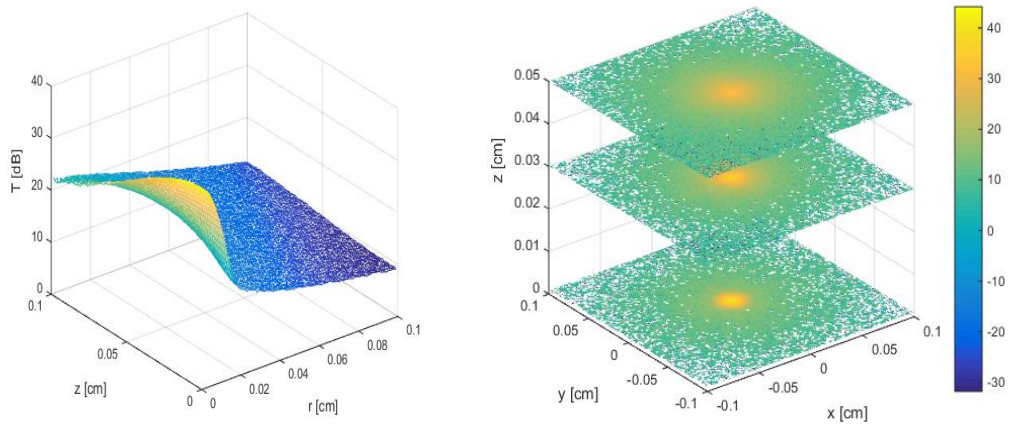

a) b)

Fig. 14 Beam with a Gaussian distribution and a radius of 0.1 cm in muscle tissue

The results indicate that the density decreases slightly at a depth of 0.03 cm but at the same time a scattering of the beam is observed. Fig. 14b shows the density of the transmission in the three cross-sections of the tissue. An expansion of the beam upon penetration into the tissue and reduction of its intensity can also be observed. These processes are less pronounced as compared to the penetration in the liver, but are more pronounced compared to the penetration in the blood. At a depth of 0.05 cm the beam retains its shape, but is with reduced intensity and considerably scattered.

Fig. 15a shows the dependence of the density of the transmission of photons in the muscle tissue, expressed in decibels, according to the penetration depth (on the *z* axis) and the radius of the distance from the *z* axis. The modelling was performed for a focused Gaussian beam entering into the tissue at a point with coordinates (0, 0, 0).

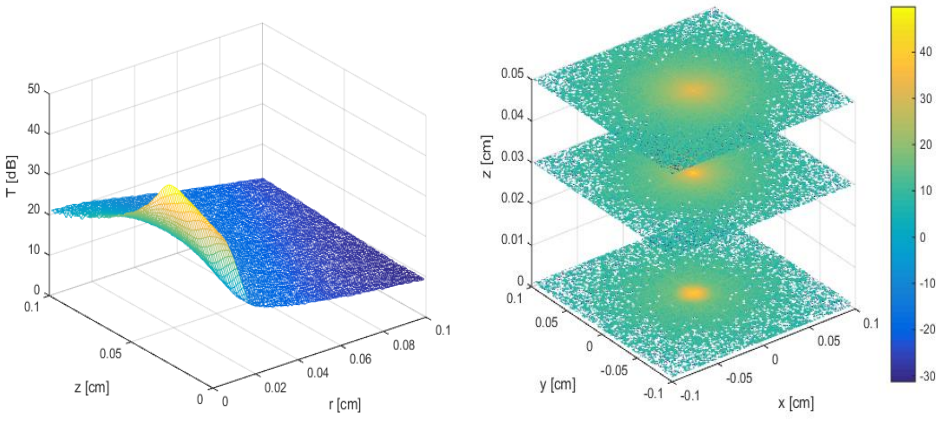

a) b)

Fig. 15 Focused Gaussian beam in muscle tissue

The results indicate that the density decreases with increasing of the penetration depth, while at the same time scattering of the beam is observed. Fig. 15b shows the density of the transmission in the three cross-sections. The results show that upon penetration in the muscle, a focusing of the beam at a depth of 0.03 cm is also observed.

Fig. 16 shows the density contours of the transmission of photons in muscle tissue at levels 37 dB, 30 dB, 27 dB, 23 dB and 13 dB for a single beam, a uniform beam with a radius of 0.1 cm, a beam with Gaussian distribution of 0.1 cm and a focused Gaussian beam depending on the penetration depth (on the *z* axis) and the radius of the distance from the *z* axis.

The comparison of the results obtained with the previous results confirm the conclusion drawn so far that the scattering of the beams in the muscle tissue is greater in comparison with that in the blood, but is less than that in the liver. As for the previous tissues, the closest to the penetration of a single beam is the focused Gaussian beam.

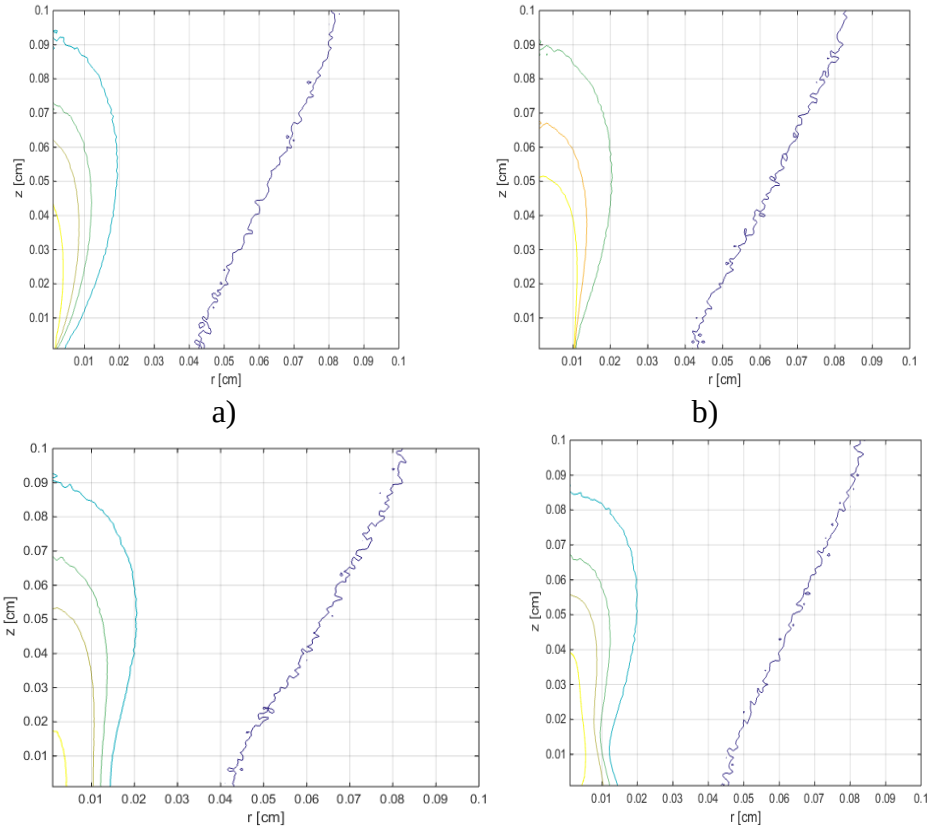

Fig. 16 Density distribution of the photons transmission in muscle tissue of:
a) a single beam; b) a uniform beam with a radius of 0.1 cm;
c) a beam with a Gaussian distribution and a radius of 0.1 cm; d) a focused Gaussian beam.

In both beams the density level of the transmission of photons of 37 dB on the *z* axis is observed at depths of approximately 0.04 cm. For the uniform beam, the depth at which such level is observed is slightly above 0.04 cm, while for the Gaussian beam it is slightly below 0.02 cm.

The analysis of the results shows that the uniform beam penetrates the deepest and has the greatest width. The Gaussian beam has the smallest depth of penetration and the most precise targeting is obtained with the focused Gaussian beam. The results obtained clearly demonstrate the significant influence of the type of tissue on the penetration depth and scattering of the beams. The considered method allows to make a preliminary assessment of the degree of penetration and area of impact on different types of tissues.

Conclusion

The nature of the interaction of laser radiation with biological tissues depends on the absorption coefficient for a particular wavelength. The considered modified Monte-Carlo method has several advantages. This method is applicable to media with different geometries and it produces three-dimensional information about the distribution of the beam into the tissue. With the launch of 1 million photons the error of the method does not exceed 1% of the value obtained.

The developed model takes into account the following characteristics of interaction of laser radiation and biological tissues:

- ✓ the reflection of laser radiation from the surface;
- ✓ attenuation of the laser beam in the structure;
- ✓ the scattering of the laser beam in the tissue;
- ✓ the dependence of the optical and thermal properties of the types of tissue included in the structure.

This model is based on numerical experiments which allow for more detailed study of the influence of different laser parameters, such as power density, time of impact, wavelength on the treated tissue (thermal conductivity, specific heat, density, scattering coefficient) and shows the extent of influence of the wavelength of the laser beam on the effect from the impact, which would allow to reduce the thermal effect on the surrounding bio-tissue and as a result, to reduce significantly the biological damage to the structures.

References

1. Airapetian V. S., O. K. Ushakov (2012). Lasers Physics, Novosibirsk (in Russian).
2. Belikov A. V., A. V. Skripnik (2008). Laser Biomedical Technologies. Part 1, Saint Petersburg (in Russian).
3. Born M., E. Wolf (1999). Principles of Optics, 7th Ed., Cambridge University Press, Cambridge.
4. Gardner C. M., A. J. Welch (1992). Improvements in the Accuracy and Statistical Variance of the Monte Carlo Simulation of Light Distribution in Tissue, Proceeding SPIE 1646, Laser-Tissue Interaction III, 400-409.
5. Hecht E. (2002). Optics, 4th Ed., Addison Wesley Longman, Inc., USA.
6. Ji W., J. Wang (2016). Detection Algorithm of a Heat-transfer System Based on Pennes Bio-heat Transfer Formula Processing, Int J Bioautomation, 20(2), 227-236.
7. Mermeklieva E., M. Matveev (2017). Electrophysiological Methods for Study of Changes in Visual Analyzer in Patients with Diabetes Mellitus, Int J Bioautomation, 21(1), 69-102.
8. Moraes L. P. B., I. Burchett, S. Nicholls, E. Paton, E. Forward, G. B. Fogarty (2017). Large Solitary Distant Metastasis of Cutaneous Squamous Cell Carcinoma to Skin Graft Site with Complete Response Following Definitive Radiotherapy, Int J Bioautomation, 21(1), 103-108.
9. Prahl S. A., M. Keijzer, S. L. Jacques, A. J. Welch (1989). A Monte Carlo Model of Light Propagation in Tissue, SPIE Proceedings of Dosimetry of Laser Radiation in Medicine and Biology, IS 5, 102-111.
10. Pushkareva A. E. (2008). Methods of Mathematical Modeling in the Optics of Biotissues, Saint Petersburg (in Russian).
11. Skipetrov S. E., S. S. Chesnokov (1998). Analysis, by the Monte Carlo Method, of the Validity of the Diffusion Approximation in a Study of Dynamic Multiple Scattering of Light in Randomly Inhomogeneous Media, Quantum Electronics, 25(8), 753-757 (in Russian).

12. Shcherbakov Y. N., A. N. Yakunin (1992). Irregular Triangular Finite Element Adaptive Grid-design Method and Its Applications, Mathematical Modelling, 4(4), 109-118 (in Russian).
13. Stranadko E. F. (1993). Current Possibilities, Problems and Perspectives of Photodynamic Therapy in Oncology, Laser Market, 7-8, 22-23 (in Russian).
14. Tuchin V. V., S. R. Utz, I. V. Yaroslavsky (1994). Tissue Optics, Light Distribution, and Spectroscopy, Optical Engineering, 33(10), 3178-3188.
15. Tuchin V. V. (1993). Skin Optics: Modeling of Light Transport and Measuring of Optical Parameters, In: Muller G., B. Chance, R. Alfano et al. (Eds.), Medical Optical Tomography: Functional Imaging and Monitoring, Proceeding SPIE, 10311, 234-258.
16. Wang L., S. L. Jacques (1992). Monte Carlo Modeling of Light Transport in Multi-layered Tissues in Standard C, University of Texas, Houston, USA.
17. Witt A. N. (1977). Multiple Scattering in Reflection Nebulae. I. A Monte Carlo Approach, The Astrophysical Journal Supplement Series, 35, 1-6.
18. Zhang J. (2017). The Application in Edge Detection of Medical Image Based on the Improved B-spline Wavelet Transform, Int J Bioautomation, 21(3), 269-278.

Assoc. Prof. Teodora Petrova, Ph.D.
E-mail: teodorapetrova33@abv.bg

Teodora Petrova is an Associate Professor in the Faculty of Aviation at "Vasil Levski" National Military University. She received her M.Sc. degree in Communication Technique and Technologies in 2002 from the "Angel Kanchev" University of Ruse and Ph.D. degree in Radiolocation and Radionavigation in 2009. She is the author of two monographs and more than 20 articles. Her research interests are in the field of lasers application in medicine.

Assoc. Prof. Zhivo Petrov, Ph.D.
E-mail: zhbpetrov@nvu.bg

Zhivo Petrov is an Associate Professor in the Faculty of Aviation at "Vasil Levski" National Military University. He received his M.Sc. degree in Radio and Television Engineering in 1994 from Bulgarian Air Force Academy "Georgi Benkovski" and Ph.D. degree in Radiolocation and Radionavigation in 2011. Hi is the author of one monograph and more than 20 articles. His research interests are in the field of radiolocation, navigation and avionics.